

Improving the Properties of Bacterial *R*-Selective Hydroxynitrile Lyases for Industrial Applications

Romana Wiedner,^[a] Bettina Kothbauer,^[a] Tea Pavkov-Keller,^[a] Mandana Gruber-Khadjawi,^[a] Karl Gruber,^[a, b] Helmut Schwab,^[a, c] and Kerstin Steiner^{*[a]}

Hydroxynitrile lyases (HNLs) catalyse the reversible cleavage of cyanohydrins to carbonyl compounds and HCN. The recent discovery of bacterial HNLs with a cupin fold gave rise to a new promising class of these enzymes. They are interesting candidates for the synthesis of cyanohydrins on an industrial scale owing to their high expression levels in *Escherichia coli*. The activity and enantioselectivity of the manganese-dependent HNL from *Granulicella tundricola* (GtHNL) were significantly improved by site-saturation mutagenesis of active site amino

acids. The combination of beneficial mutations resulted in a variant with 490-fold higher specific activity in comparison to the wild-type enzyme. More importantly, GtHNL-A40H/V42T/Q110H is a highly competitive alternative for the synthesis of chiral cyanohydrins, such as 2-chlorobenzaldehyde cyanohydrin, (*R*)-2-hydroxy-4-phenylbutyronitrile, and (*R*)-2-hydroxy-4-phenyl-3-butene nitrile, which serve as intermediates for the synthesis of pharmaceuticals.

Introduction

Hydroxynitrile lyases (HNLs) catalyse the stereoselective cleavage of cyanohydrins. More importantly, they are valuable tools in biocatalysis owing to their ability to synthesise chiral α -cyanohydrins through a C–C bond forming condensation reaction. A chiral centre is (potentially) formed, the carbon chain is elongated by one carbon atom, and an additional versatile functional group—the nitrile—is introduced into the molecule. Enantiopure cyanohydrins are versatile building blocks and intermediates that serve as starting materials for many enzymatic and chemical follow-up reactions, which find application in pharmaceutical, agrochemical, and cosmetic industries.^[1–4] To meet the requirements for industrial applications, HNLs need to fulfil several criteria in addition to high enantioselectivity: 1) availability of sufficient quantities of proteins with consistent quality and batch-to-batch reproducibility at low cost, 2) broad substrate scope, 3) high stability at acidic pH and high solvent stability, and 4) activity at low temperatures [as the unselective chemical background reaction is significantly suppressed at

low pH (<4.5), at low temperature, and in the absence of water].^[5]

A number of *R*- and *S*-selective HNLs have been identified so far (see tables in related reviews^[4,6]); however, only a few of them can be heterologously expressed in sufficient amounts either in *Escherichia coli* or in *Pichia pastoris*. Bacterial HNLs with a cupin fold, which have recently been discovered, can be expressed in *E. coli* in exceptionally high yield.^[7–9] The bacterial manganese-dependent HNL from *Granulicella tundricola* (GtHNL) was characterised in detail, and its structure was solved.^[7,10] GtHNL catalysed the synthesis of (*R*)-mandelonitrile from benzaldehyde and HCN with 80% conversion and 90% ee, which is not sufficient for industrial applications, but is a promising starting point for protein engineering approaches.

In recent years, enzyme engineering by either random or directed methods was applied to HNLs to increase their stability (at elevated temperature, at acidic pH, or in organic solvents), to broaden their substrate scope, to reverse or increase their enantioselectivity, and to increase their expression levels.^[4,6,11–13] The stability of the *R*-selective AtHNL from *Arabidopsis thaliana* at acidic pH was improved by one pH unit by exchanging eleven surface amino acids with the corresponding amino acids of the *S*-selective MeHNL from *Manihot esculenta*, which belongs to the same fold and is more stable.^[14] Moreover, the activity, enantioselectivity, and substrate scope of the *R*-selective PaHNL5 from *Prunus amygdalus* were significantly improved by enzyme engineering.^[15–18]

The aim of the present work was the engineering of GtHNL to improve its activity and stability at low pH as well as to broaden its substrate scope. For this purpose, random mutagenesis of the entire coding region and site-saturation mutagenesis of active site amino acids (designed evolution) were performed. Promising variants were tested as catalysts for the

[a] Dr. R. Wiedner, B. Kothbauer, Dr. T. Pavkov-Keller, Dr. M. Gruber-Khadjawi, Prof. K. Gruber, Prof. H. Schwab, Dr. K. Steiner
ACIB, Austrian Centre of Industrial Biotechnology GmbH
Petersgasse 14, 8010 Graz (Austria)
Fax: (+43) 3168739346
E-mail: kerstin.steiner@acib.at

[b] Prof. K. Gruber
Institute of Molecular Biosciences
University of Graz
Humboldtstraße 50, 8010 Graz (Austria)

[c] Prof. H. Schwab
Institute of Molecular Biotechnology
TU Graz
Petersgasse 14, 8010 Graz (Austria)

Supporting information for this article is available on the WWW under <http://dx.doi.org/10.1002/cctc.201402742>.

synthesis of mandelonitrile and several other industrially relevant cyanohydrins.

Results and Discussion

Engineering of cupin HNLs

GtHNL catalysed the synthesis of *R*-selective mandelonitrile in a biphasic reaction system [100 mM sodium acetate buffer, pH 4.0, methyl *tert*-butyl ether (MTBE) (1:2) containing 0.5 M benzaldehyde and 2 M HCN, 1000 rpm, 5 °C, 24 h] with a good conversion of 80% and promising *ee* of 90%.^[7] Unfortunately, the substrate scope of the wild-type enzyme was rather limited. Thus, GtHNL had to be improved with respect to its general activity and substrate scope by protein engineering. The activity and stability at acidic pH were targeted to suppress the unspecific chemical background reaction, which significantly reduces the enantiopurity of the reaction products. Different mutant libraries were created by random mutagenesis, including either the whole coding region or three parts of the gene excluding the metal-binding amino acids (Figure S1). In addition, site-saturation mutagenesis of active site amino acids was performed.

Screening of the libraries for improved HNL activity and stability at acidic pH

Whole gene and fragment random mutagenesis of GtHNL resulted in reasonable mutation rates (corresponding to one to three amino acid mutations per gene for the whole gene library). In total, 22 000 variants obtained from different random libraries were screened for improved activity and stability towards (*R*)-mandelonitrile at pH 3.5 with a colony-based colorimetric HNL assay,^[19] detecting HCN released during cyanogenesis (Figure S2). From 122 preliminary selected hits, 30 variants with apparently improved activity in the cleavage of (*R*)-mandelonitrile were identified after rescreening. Five variants harboured an amino acid exchange at position Q110 and one variant had an amino acid exchange at position V42—the two positions that were also targeted in site-saturation mutagenesis.

In addition, the site-saturation mutagenesis libraries (264 variants of each) of eight active site positions (A40, V42, F44, T50, L61, H96, H106, and Q110, lining the cavity of the proposed active site;^[7] see Figure 1) were screened for improved activity towards (*R*)-mandelonitrile. The libraries at position F44, T50, L61, and H96 contained no improved variants, whereas two hits were obtained from the A40 library, one improved variant resulted from the V42 library, and two and one hit were discovered in the H106 and Q110 libraries, respectively (Table S1).

Confirmation of improved HNL activity and stability at acidic pH

The most promising variants obtained from both approaches were recloned into a pET26b expression vector and expressed in shake flasks under standard conditions.^[7] They were all well

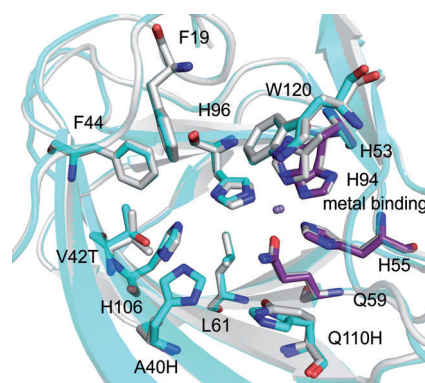


Figure 1. Crystal structure of GtHNL-A40H/V42T/Q110H superimposed with that of GtHNL-WT (PDB entry 4bif; grey). Active site amino acids are shown as sticks (—: WT; GtHNL-A40H/V42T/Q110H: —: metal-binding amino acids, —: active site amino acids). The figure was prepared by using the program PyMOL.

expressed as soluble proteins at the same level as the wild-type GtHNL (GtHNL-WT; Figure S3). As the hits were detected in a colony assay, their activity and pH stability had to be confirmed in the cyanogenesis of (*R*)-mandelonitrile at different pH values by using purified GtHNL variants in a quantitative photometric assay.

Even though many of the chosen variants demonstrated increased activities than GtHNL-WT, hits from site-saturation mutagenesis (Table 1) were significantly more active than most hits from random mutagenesis (Figure S4), which were mainly in the activity range of the wild-type enzyme.

Table 1. Specific activities of different GtHNL variants obtained from site-saturation mutagenesis libraries in different buffers at various pH values (100 mM citrate/phosphate and oxalate buffer at pH 5.0 and 5.5) with 18 mM (*R*)-mandelonitrile as the substrate.^[a]

GtHNL variant	Specific activity [U mg ⁻¹]			
	Oxalate buffer		Citrate/phosphate buffer	
	pH 5.0	pH 5.5	pH 5.0	pH 5.5
WT	0.20 ± 0.00	0.29 ± 0.01	0.12 ± 0.02	0.28 ± 0.03
A40H	3.21 ± 0.13	3.69 ± 0.06	0.48 ± 0.04	3.34 ± 0.10
V42T	4.45 ± 0.30	5.03 ± 0.20	0.57 ± 0.01	1.83 ± 0.01
Q110H	0.70 ± 0.01	1.37 ± 0.14	0.11 ± 0.01	0.35 ± 0.03

[a] Depending on the activity of the variant, different protein concentrations (from 5 μg mL⁻¹ to 1 mg mL⁻¹) were used. The increase in benzaldehyde absorption was followed at 280 nm in a plate reader.

The best variant obtained from random mutagenesis (GtHNL-F29L/L36R/V42A) exhibited an approximately 5 times higher specific activity than GtHNL-WT, whereas GtHNL-A40H, GtHNL-V42T, and GtHNL-Q110H showed 12, 17, and 5 times higher specific activities at pH 5.5 in oxalate buffer than the wild-type enzyme. However, all variants showed substantially reduced or even no activity at pH 4.5 and 4.0 (data not shown). In many cases, denaturation of the enzymes was visible as precipitation. This finding was confirmed by thermal shift measurements, which showed a significant decrease in

the melting temperature (T_m) of GtHNL-WT and all variants in different buffers, from pH 5.5 (e.g., sodium oxalate: T_m values in the range of 60–70 °C, depending on the variant) to pH 4.5 (at which several variants were already unfolded at the start of the measurement at 20 °C or had T_m values in the range of 35–50 °C) and pH 4.0 (at which all proteins were unfolded at the beginning, except for GtHNL-WT and variants A40H and A40R). Most variants were slightly more stable in citrate/phosphate buffer and sodium acetate buffer than in sodium oxalate buffer. However, none of the variants had a higher melting temperature than the wild-type enzyme in any of the tested buffers. These results reveal that colony-based assays have to be handled with care with regard to pH stability. Although the colonies were treated with freeze–thaw cycles to break the cells and enable equilibration at low pH, the results indicate that either the cells were not sufficiently broken and the pH of the unbroken cells was higher than assumed or the HNL protein was still stabilised or protected against the low pH by cell debris.

Activity of the variants in the synthesis of (*R*)-mandelonitrile

First experiments for the synthesis of (*R*)-mandelonitrile with cleared lysate of *E. coli* showed that several variants demonstrated improved conversion and/or enantioselectivity in comparison to GtHNL-WT (Table 2).

GtHNL variant	Conversion [%]	ee (<i>R</i>) [%]
I3L/T20A	96.5	94.1
I25M/L36Q	92.4	93.6
I109L/A117V	98.4	96.3
A40H	99	87.9
A40R	97.6	94.5
H106N	38.4	73.7
H106Y	97.9	n.d. ^[b]
Q110H	95.4	95.4
V42T	98.8	96.3
WT	84.6	88.7

[a] Reaction conditions: two-phase system consisting of 500 μ L of cell-free lysate (22.5 mg of the total protein with \approx 50% cupin in 100 mM sodium acetate buffer, pH 4.0) as the aqueous phase and 1 mL of MTBE containing 0.5 M benzaldehyde and 2 M HCN as the organic phase, 1000 rpm, $T = 5^\circ\text{C}$, $t = 24$ h. [b] Not detected.

Most variants that resulted from the random libraries showed similar conversions and enantioselectivities as did GtHNL-WT (Figure S5). However, significantly increased conversion and ee values were obtained with GtHNL-I3L/T20A, GtHNL-I25M/L36Q, and GtHNL-I109L/A117V (Table 2). Improved conversions and enantioselectivities were again observed with several variants from site-saturation mutagenesis libraries, that is, GtHNL-A40H, GtHNL-A40R, GtHNL-V42T, and GtHNL-Q110H. Surprisingly, GtHNL-H106N showed substantially reduced con-

version (38.4%) and reduced ee (73.7%). GtHNL-H106Y converted 97.9% of benzaldehyde in 24 h, but completely lost its enantioselectivity.

Screening of random libraries for activity towards racemic 2-chloromandelonitrile

(*R*)-2-Chloromandelonitrile is a precursor of (*R*)-2-chloromandelic acid, a key intermediate in the synthesis of an antiplatelet agent, clopidogrel. The synthesis of (*R*)-2-chloromandelonitrile from 2-chlorobenzaldehyde has previously been improved by rational engineering of HNL isoenzyme 5 from *P. amygdalus*.^[15] However, PaHNL5 can be overexpressed only in *P. pastoris*, and an enzyme catalyst expressed in *E. coli* in high yield would be preferable. The screening of the whole gene random library for activity towards (*R/S*)-2-chloromandelonitrile originated nine variants that showed increased activity. Seven of these variants shared a variation at position F19, F19V, or L as a single amino acid exchange or in combination with silent mutations or additional amino acid exchanges (data not shown). The two remaining hits harboured the amino acid exchange at W120R. These candidates were not discovered during the screening of the same library with the (*R*)-mandelonitrile substrate. This finding was later confirmed by the fact that purified GtHNL-F19V and -W120R were both less active in the cyanogenesis of (*R*)-mandelonitrile in the plate reader assay as compared with the wild-type enzyme (data not shown). Whereas GtHNL-WT was almost inactive with 2-chloromandelonitrile (*S* enantiomer: no activity; *R* enantiomer: 0.03 U mg^{-1} in citrate/phosphate buffer, pH 5.5), GtHNL-F19V was particularly active towards (*S*)-2-chloromandelonitrile (*S* enantiomer: 2.08 U mg^{-1} ; *R* enantiomer: 0.39 U mg^{-1}) and GtHNL-W120R showed some activity towards both enantiomers (*S* enantiomer: 0.25 U mg^{-1} ; *R* enantiomer: 0.13 U mg^{-1}).

In the synthesis of 2-chloromandelonitrile with cell-free lysate, GtHNL-F19V and GtHNL-F19V/F88V showed higher conversions (97.8 and 94.7%, respectively) than GtHNL-WT (89% conversion with 36.1% ee (*R*)) but exhibited inverted enantioselectivities (26 and 33.9% ee (*S*), respectively). Conversely, the variant W120R converted 99.8% of the substrate to (*R*)-2-chloromandelonitrile with a significantly improved ee of 71.9% in comparison to the wild-type enzyme. Both variants were significantly less active and enantioselective than GtHNL-WT in the synthesis of mandelonitrile (Figure S5). The results suggest that the choice of the substrate in the screening affects the result: because racemic 2-chloromandelonitrile was used as the screening substrate, variants with higher activity were identified independent of their enantioselectivity. W120 is located in the active site close to the metal-binding site (Figure 1). Assuming that the carbonyl group of 2-chlorobenzaldehyde points towards the metal, the chlorine at the *ortho* position could come in close contact with the bulky tryptophan side chain and thus steric hindrance could cause a slightly different binding position, which resulted in lower conversion and enantioselectivity of the wild-type enzyme (Figure S6). A mutation at this position creates more space for the chlorine, and the positively charged arginine could interact with the electroneg-

ative chlorine. F19 is located in the already open entrance region of the active site of GtHNL. The exchange of F19 with the smaller amino acids valine or leucine could enable the entry of larger substrates; however, the larger space can favour non-productive binding or binding in a different orientation, which results in reduced or inverted enantioselectivity.

Combination of beneficial mutations

The beneficial mutations identified in the site-saturation mutagenesis libraries (A40H, A40R, V42T, and Q110H) were combined. Whereas most of the double variants showed only a slight increase in conversion and/or enantioselectivity in comparison to the single variants, the double mutant GtHNL-A40H/V42T was significantly better (data not shown). Most promising, however, was the triple mutant GtHNL-A40H/V42T/Q110H, which had already achieved nearly full conversion of benzaldehyde after 2 h (98%), with an excellent *ee* (*R*) of >99.9% (Figure 2).

Moreover, purified GtHNL-A40H/V42T/Q110H showed a specific activity of $137 \pm 9.95 \text{ U mg}^{-1}$ in the cyanogenesis of 18 mM (*R*)-mandelonitrile in citrate/phosphate buffer, pH 5.5, which corresponds to an approximately 490-fold increase in activity compared with GtHNL-WT under the same reaction conditions. In contrast to GtHNL-WT, purified GtHNL-A40H/V42T/Q110H showed significant residual activity even at pH 4.0 and 4.5 (2.3 ± 0.04 and $10.3 \pm 0.09 \text{ U mg}^{-1}$, respectively). Kinetic measurements of purified GtHNL-A40H/V42T/Q110H and GtHNL-WT were performed in

sodium oxalate buffer, pH 5.5, which revealed a Michaelis constant (K_m) of $12.8 \pm 0.4 \text{ mM}$ and a turnover number (k_{cat}) of $51 \pm 1.2 \text{ s}^{-1}$ for GtHNL-A40H/V42T/Q110H compared with a K_m of $6.1 \pm 0.2 \text{ mM}$ and a k_{cat} of $0.075 \pm 0.003 \text{ s}^{-1}$ for GtHNL-WT.

Substrate scope of GtHNL-A40H/V42T/Q110H

Purified GtHNL-A40H/V42T/Q110H was subjected to substrate screening in the synthesis of cyanohydrins including several aldehydes (Table 3). Hydroxypivaldehyde was tested at pH 2.4 and 4.0, but was not converted by the variant, which was not

Table 3. Conversion and enantioselectivity of purified GtHNL-A40H/V42T/Q110H towards different aldehydes after 2 and 24 h.^[a]

Substrate ^[b]	<i>t</i> = 2 h				<i>t</i> = 24 h			
	Mutant		WT		Mutant		WT	
	Conv. [%]	<i>ee</i> [%]	Conv. [%]	<i>ee</i> [%]	Conv. [%]	<i>ee</i> [%]	Conv. [%]	<i>ee</i> [%]
1a	87.9	>99.9	n.x. ^[c]	n.x.	98.6	99.8	50.0	89.3
2a	62.1	99.1	24.5	14.9	99.9	99.4	60.5	23.8
3a	85.4	97.9	26.4	-13.9	94.7	98.5	78.9	-13.5
4a	70.7	>99.9	17.4	>99.9	97.0	>99.9	21.8	77.8
5a	98.2	99.5 ^[d]	77.9	74.8 ^[d]	98.3	98.1 ^[d]	95.8	72.2 ^[d]
6a	n.d. ^[e]	n.d.	n.d.	n.d.	n.d.	n.d.	n.d.	n.d.

[a] Reaction conditions: two-phase system consisting of 500 μL of purified enzyme [4.7 mg of GtHNL-A40H/V42T/Q110H (mutant) and 3.7 mg of GtHNL-WT in 100 mM sodium acetate, pH 4.0] as the aqueous phase and 1 mL of MTBE containing 0.5 M aldehyde and 2 M HCN as the organic phase, 1000 rpm, $T = 5^\circ\text{C}$. [b] **1a** = benzaldehyde; **2a** = 2-chlorobenzaldehyde; **3a** = 3-phenylpropanal; **4a** = 3-phenylprop-2-enal; **5a** = 2-furylaldehyde; **6a** = hydroxypivaldehyde. [c] Not determined. [d] Change of product configuration as a consequence of the Cahn-Ingold-Prelog rule. [e] Not detected.

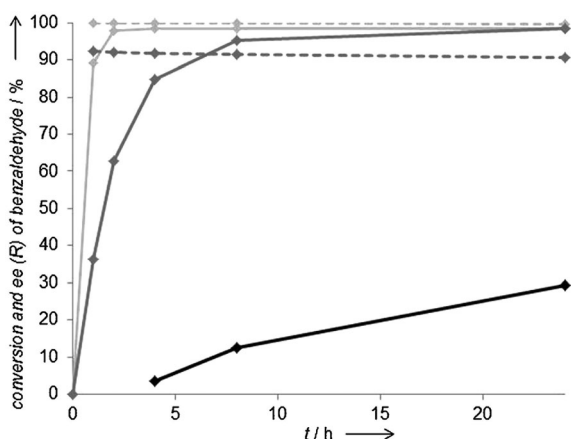


Figure 2. Conversion of benzaldehyde and *ee* (*R*) obtained with GtHNL-WT (grey) and GtHNL-A40H/V42T/Q110H (light grey) at different time points. Conversions are shown as solid lines, and *ee* values are shown as dashed lines. Reaction conditions: two-phase system consisting of 500 μL of cell-free lysate (22.5 mg total protein with $\approx 50\%$ cupin in 100 mM sodium acetate buffer, pH 4.0) as the aqueous phase and 1 mL of MTBE containing 0.5 M benzaldehyde and 2 M HCN as the organic phase, 1000 rpm, $T = 5^\circ\text{C}$. The product (black line) of the negative control (empty pET26b vector) is racemic.

surprising because at pH 4.0 it is mainly found as a dimer and the enzyme was not active at pH 2.4. For all other substrates, excellent enantioselectivities and good to excellent conversions were achieved (Table 3). Reducing the applied amount of the enzyme to a tenth still resulted in excellent enantioselectivities but with reduced conversion after 2 h and full conversion after 24 h (Table S2).

Compared to literature data, the excellent enantioselectivity in particular makes GtHNL-A40H/V42T/Q110H a highly competitive alternative for the synthesis of chiral cyanohydrins. The *R*-selective AtHNL from *A. thaliana* resulted in 99% conversion of 3-phenylpropanal but only 68% *ee* after 22 h (however with only 50 mM aldehyde and 0.25 M HCN).^[20] While PaHNL-WT showed moderate to excellent conversions and enantioselectivities depending on the substrate, several variants of PaHNL were created in recent years that achieved excellent conversions and enantioselectivities (e.g., 2-chlorobenzaldehyde: 98.5%; 3-phenylpropanal: 96.7%; 3-phenylprop-2-enal: 97.6%).^[15, 16, 18, 21, 22]

Structural analysis of GtHNL-A40H/V42T/Q110H

The GtHNL-A40H/V42T/Q110H variant was crystallised in a different space group as compared with the wild-type enzyme,^[7] and its structure was determined at 2.1 Å resolution (Table S3). The asymmetric unit contains 20 molecules of the variant arranged in five tetramers. The tetramers as well as the overall fold of the individual chains are conserved in the variant enzyme, as indicated by the overall root mean square deviation (for C α atoms) between the two structures, which does not exceed 0.35 Å when individual chains (or tetramers) are superimposed (Figure 1).

The active site structure, however, demonstrates profound changes that correlate with the measured activity increase in the variant. With three amino acid substitutions, a much narrower cavity is created in the vicinity of the manganese-binding site (Figure 3 a,b). This cavity is more hydrophilic than in the wild-type enzyme and possibly provides additional positive charges through His40 and His110 (Figure 3 c,d). The newly in-

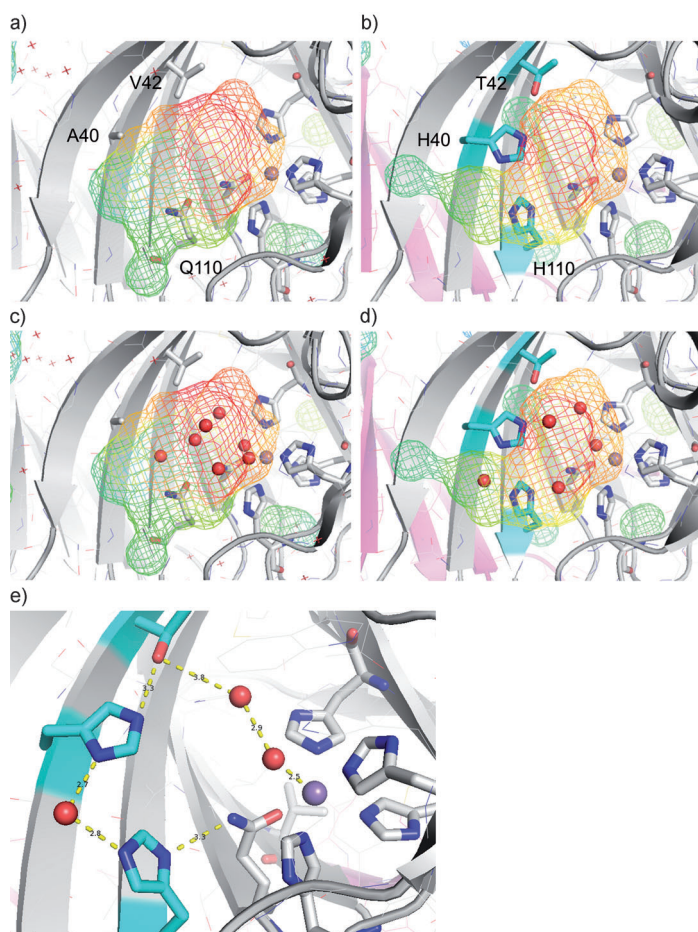


Figure 3. Structural analysis of the active site of GtHNL-A40H/V42T/Q110H (b,d: —: exchanged amino acids) compared with GtHNL-WT (a,c: —). The manganese ion is depicted as a purple non-bonded sphere. a,b) Comparison of the size and shape of the cavities that harbour the active site of the WT and the variant enzymes, respectively, depicted as a meshed cloud. c,d) Comparison of the distribution of water molecules in the active sites (red non-bonded spheres). e) Zoom-in of the network of hydrogen bonds in the active site of GtHNL-A40H/V42T/Q110H. The figures were prepared with the program PyMOL.

roduced residues are positioned in such a way that a network of hydrogen bonds is formed (Figure 3e), which thus defines their own conformations as well as the positions of water molecules in the active sites.

The minimal requirements for HNL activity are the presence of a catalytic base and a positive charge or general positive electrostatic potential in the binding pocket.^[23] By assuming that the hydroxyl group of the cyanohydrin (or the carbonyl oxygen of the aldehyde or ketone) is bound to the manganese ion, we propose that the negative charge at the cyano group or cyanide is better stabilised by the additional positive charges provided by the two histidine residues in comparison to the wild-type enzyme (Figure S6).

Transfer of beneficial mutations to the cupin HNL from *Acidobacterium capsulatum*

To investigate the general importance of these amino acids in the active site of HNLs with a cupin fold, the beneficial mutations A40H, V42T, and Q110H were transferred as single and triple mutations to a recently discovered highly similar cupin HNL from *Acidobacterium capsulatum* ATCC 51196 (A cHNL),^[9] and tested in the cyanogenesis and synthesis of (*R*)-mandelonitrile (Tables S4 and S5). GtHNL and A cHNL share 77% sequence identity, and most active site amino acids such as A40, V42, and Q110 are identical. The purified A cHNL triple mutant A cHNL -A40H/V42T/Q110H showed a specific activity of $139 \pm 11.2 \text{ U mg}^{-1}$ in the cyanogenesis of 18 mM (*R*)-mandelonitrile in citrate/phosphate buffer, pH 5.5, which is identical to that of GtHNL-A40H/V42T/Q110H. Moreover, purified A cHNL -A40H/V42T/Q110H was investigated in the bioconversion of benzaldehyde and showed 99.4% conversion and 99.7% ee (*R*) after 24 h.

Conclusions

Random and site-saturation mutagenesis of the manganese-dependent hydroxynitrile lyase (HNL) from *Granulicella tundricola* (GtHNL) originated a remarkable number of variants with improved HNL activity in the cyanogenesis of (*R*)-mandelonitrile and, more importantly, in the synthesis of cyanohydrins. GtHNL-A40H/V42T/Q110H, a combinatorial variant of three beneficial amino acid exchanges in the active site, was superior to all other variants. Moreover, the general importance of these amino acids in the active site of HNLs with a cupin fold was confirmed by the successful transfer of these amino acid exchanges to another cupin HNL, the cupin HNL from *Acidobacterium capsulatum*.

The excellent enantioselectivity combined with its high expression level in *Escherichia coli* makes GtHNL-A40H/V42T/Q110H a highly competitive alternative for the synthesis of chiral cyanohydrins, such as 2-chlorobenzaldehyde cyanohydrin, (*R*)-2-hydroxy-

4-phenylbutyronitrile, and (*R*)-2-hydroxy-4-phenyl-3-butene nitrile, which serve as intermediates for the synthesis of pharmaceuticals, for example antiplatelet agents or a class of angiotensin-converting enzyme inhibitors.

Experimental Section

General

All chemicals were purchased from Sigma–Aldrich or Carl Roth GmbH, if not stated otherwise. Materials for molecular biology were obtained from Thermo Fisher Scientific, if not specifically mentioned. *E. coli* TOP10F' was used for basic cloning work and as a host for mutant libraries. *E. coli* BL21-Gold(DE3) was used for protein expression. HPLC analyses were performed on an Agilent 1100 instrument (Agilent Technologies) equipped with an autosampler, a multi-wavelength detector, and a Daicel Chiralcel OD-H column (250 mm × 4.6 mm × 5 μm; Chiral Technologies). For GC analysis, an HP 6890 GC system (Hewlett-Packard) equipped with a flame ionization detector and a CP-Chirasil-DEX CB column (25 m × 0.32 mm, 0.25 mm film; Agilent Technologies) was used.

Cloning and mutagenesis

For details of the used methods, see the Supporting Information. Random mutagenesis was performed by an error-prone polymerase chain reaction (PCR). The error rate of the polymerase was increased by the addition of MnCl₂, an increased amount of MgCl₂, and unbalanced nucleotide concentrations. The plasmid pMS470-GtHNL (codon optimised for *E. coli*^[7]) was used as the template for the amplification of the 396 bp target sequence. The PCR product was purified and recloned into pMS470Δ8^[24] by using *Nde*I and *Hind*III restriction sites. The desalted ligation mixture was transformed into *E. coli* TOP10F' cells. The average mutation rate was estimated by sequencing randomly selected variants (LGC Genomics). In addition, to exclude the metal-binding amino acids from mutagenesis, random mutagenesis libraries of three regions of the gene were constructed (Figure S1) through a standard error-prone PCR with DreamTaq DNA polymerase or through amplification with Mutazyme II (Agilent Technologies). The resulting PCR products were then used as megaprimers for the site-directed mutagenesis of pMS470-GtHNL. Site-directed and site-saturation mutagenesis of pMS470-GtHNL were performed with a single-primer reactions in parallel mutagenesis protocol.^[25] Degenerated oligonucleotides (Table S6) used for site-saturation mutagenesis contained NNK triplets at the targeted positions. Thus, a mixture of 32 mutants containing all 20 proteinogenic amino acids at respective positions was created. *Dpn*I-digested PCR products were used for the transformation of electrocompetent *E. coli* TOP10F' cells.

Improved GtHNL variants were subcloned into plasmid pET26b(+) by using *Nde*I and *Hind*III restriction sites. The beneficial mutations of GtHNL were combined and transferred to AchNL from *Acidobacterium capsulatum* ATCC 51196^[9] as single and triple mutations by using a single-primer reactions in parallel mutagenesis protocol (as described above) with pET26b(+)-GtHNL-Q110H and pET26b(+)-AchNL and then pET26b(+)-AchNL-Q110H as the template. The resulting constructs were confirmed by sequencing (LGC Genomics) and transformed into electrocompetent *E. coli* BL21-Gold(DE3) cells.

Screening of libraries

The transformants from each GtHNL random library were grown on LB agar (supplemented with 100 mg L⁻¹ of ampicillin). The colonies were transferred to 384-well plates (Nunc, Thermo Scientific) filled with 2xTY medium (55 μL per well) containing ampicillin (final 100 mg L⁻¹ per well) with a QPix picking robot (Genetix, now Molecular Devices LLC). The transformants from site-saturation mutagenesis libraries were picked into the wells of 96-well plates (filled with 100 μL of LB medium containing 100 mg L⁻¹ of ampicillin) with sterile toothpicks. *E. coli* TOP10F' cells harbouring pMS470-GtHNL or empty pMS470Δ8 plasmid were added to each plate as positive and negative controls, respectively. All plates were incubated at 37 °C overnight and were then used as templates for transferring colonies to nylon membranes (Biodyne A, 0.2 μm; Pall Life Sciences) with a pin stamp. A colony-based colorimetric filter assay, as described previously^[19] (for details, see the Supporting Information), using (*R*)-mandelonitrile or racemic 2-chloromandelonitrile as a substrate was used.

Protein expression and purification

Precultures of *E. coli* BL21-Gold(DE3) cells harbouring pET26b(+) constructs were grown in LB medium (100 mL) supplemented with kanamycin (40 mg L⁻¹) at 37 °C overnight. They were used for the inoculation of LB medium (330 mL) containing kanamycin (40 mg L⁻¹) to an optical density at λ = 600 nm (OD₆₀₀) of approximately 0.03. Cultivation was performed at 37 °C until an OD₆₀₀ of 0.6–0.8 was reached. Protein expression was induced by adding isopropyl-β-D-thiogalactoside (0.1 mM), and cultivation was continued at 25 °C for 20 h. Moreover, MnCl₂ (0.1 mM) was added to the cultures at the induction time. Cells were harvested at 3600g, 20 min, and 4 °C; resuspended in sodium phosphate buffer (30 mL, 10 mM, pH 7.0); and disrupted by sonication (Sonifier S-250, Branson Ultrasonics Corporation; 80% duty cycle, output control 8) for 6 min under continuous cooling. Cell-free lysates were obtained by centrifugation (48 000g, 1 h, 4 °C). For cyanohydrin synthesis, cleared lysates were concentrated to 50 mg mL⁻¹ with Vivaspin 20 centrifugal concentrators (10 kDa molecular mass cut-off; Sartorius). The lysates were stored at –20 °C.

For purification of GtHNL-WT and variants thereof, and of AchNL-WT and variants thereof, the enzymes were expressed as described above and the cell pellets were resuspended in buffer A (50 mM BIS-TRIS buffer, 30 mM NaCl) and lysed as described above. The pH of the buffer was set according to the theoretical isoelectric point of the wild-type enzyme and variants (Table S7), which was calculated by using the program ProtParam.^[26] Cleared lysates were purified by using anion-exchange chromatography with Q Sepharose Fast Flow columns (HiTrap Q FF, 3 × 5 mL; GE Healthcare, Uppsala, Sweden) applying a step of 10% (or 20% for GtHNL-W120R, GtHNL-K93E, and GtHNL-I3T variants) buffer B (50 mM BIS-TRIS buffer, 1 M NaCl, the same pH as the respective buffer A). The fractions were analysed by using sodium dodecyl sulfate polyacrylamide gel electrophoresis, pooled, and then concentrated. GtHNL-WT and GtHNL-A40H/V42T/Q110H were further purified by using size-exclusion chromatography with a HiLoad 16/600 Superdex 75 pg column (125 mL; GE Healthcare). Proteins were eluted with sodium phosphate buffer (50 mM, pH 7.0) containing NaCl (100 mM). GtHNL-A40H/V42T/Q110H used for crystallography was eluted in TRIS-HCl (20 mM; pH 7.0) containing NaCl (200 mM). The fractions were analysed by using sodium dodecyl sulfate polyacrylamide gel electrophoresis, and those containing the desired protein were pooled and concentrated to 10–20 mg mL⁻¹.

HNL activity assay

The activity of the enzymes in the cyanogenesis of (*R*)-mandelonitrile or (*R*)- and (*S*)-chloromandelonitrile was determined spectrophotometrically by following the increase in benzaldehyde and 2-chlorobenzaldehyde absorption at 280 and 300 nm, respectively, in a plate reader at 25 °C. The reaction buffer (130 μ L; either 100 mM citrate/phosphate buffer, pH 4.0, 4.5, 5.0, and 5.5; 100 mM sodium oxalate buffer, pH 4.0, 4.5, and 5.0; or 100 mM MES oxalate buffer, pH 5.5) was mixed with the enzyme sample (20 μ L; 1–200 μ g of the total purified protein per well), and the reaction was started by adding a cyanohydrin [50 μ L; (*R*)-mandelonitrile dissolved in 3 mM citrate/phosphate buffer, pH 3.5, or 3 mM oxalic acid, pH 2.6, or 2-chloromandelonitrile dissolved in 40% DMSO in 3 mM citrate/phosphate buffer, pH 3.2, final concentration 18 mM]. Blank reactions contained a buffer (20 μ L) instead of the enzyme sample. The blank reaction corresponded to the chemical cyanogenesis of the cyanohydrin under the respective reaction conditions. The resulting slopes ($\Delta A/\text{min}_{\text{blank}}$) were subtracted from those of the enzyme-catalysed reactions ($\Delta A/\text{min}_{\text{enzyme}}$). The activity was calculated by using the Beer–Lambert law and molar extinction coefficients $\epsilon_{280\text{ nm}} = 1.376\text{ Lmmol}^{-1}\text{ cm}^{-1}$ and $\epsilon_{300\text{ nm}} = 1.521\text{ Lmmol}^{-1}\text{ cm}^{-1}$ for benzaldehyde and 2-chlorobenzaldehyde, respectively. All measurements were performed as triplicates. The apparent kinetic data were obtained from the initial rate measurements at pH 5.5 (100 mM sodium oxalate buffer) and 25 °C by using (*R*)-mandelonitrile concentrations from 1.5 to 48 mM and with purified wild-type GtHNL (150 μ g per well) or purified GtHNL-A40H/V42T/Q110H (0.6 μ g per well), as described above.

One mandelonitrile cyanogenesis unit is defined as the amount of enzyme that catalyses the formation of 1 μ mol of benzaldehyde from mandelonitrile dissolved in aqueous buffer in 1 min at 25 °C.

Cyanohydrin synthesis

All reactions involving cyanides were performed in a well-ventilated hood equipped with an HCN detector (Dräger Pac III). The reactions were performed in two-phase systems, with the organic phase (1 mL) containing the substrate (0.5 M aldehyde), the internal standard (2% v/v triisopropylbenzene), and HCN (2 M) in MTBE. The aqueous phase (500 μ L) comprised the enzyme (cleared lysate with a total protein concentration of 45 mg mL⁻¹ containing \approx 50% cupin, or purified enzyme with a concentration of 1–10 mg mL⁻¹) in sodium acetate buffer (100 mM, pH 4.0) or sodium citrate buffer (100 mM, pH 2.4). The pH of the acidified samples was controlled before use. HCN was produced in situ and extracted in MTBE as described earlier by Okrob et al.^[27] Benzaldehyde, 2-chlorobenzaldehyde, and 2-furaldehyde were freshly distilled; hydroxypivaldehyde was monomerised by gentle heating before use. The reactions were performed in 2 mL reaction tubes on a thermomixer shaking at 1000 rpm and 5 °C. Samples were withdrawn from the organic stock solution before adding the aqueous phase as a reference, which represented the initial amount of the substrate and internal standard. For HPLC analysis of the conversion of benzaldehyde, samples of the organic phase (10 μ L) were withdrawn at appropriate time points and diluted 1:100 with HPLC eluent (*n*-heptane/*i*Pr/trifluoroacetic acid = 96:4:0.1). Chiral HPLC analysis was performed with a Daicel CHIRALCEL OD-H column) with a flow rate of 0.9 mL min⁻¹, temperature 25 °C, and UV detection at 210 and 254 nm. **1a**: retention times: triisopropylbenzene 3.8 min, benzaldehyde 7.5 min, (*S*)-mandelonitrile 29.1 min, (*R*)-mandelonitrile 30.6 min.

Alternatively, for the GC analysis of the conversion of benzaldehyde (**1a**), 2-chlorobenzaldehyde (**2a**), 3-phenylpropanal (**3a**), 3-phenylprop-2-enal (**4a**), 2-furaldehyde (**5a**), and hydroxypivaldehyde (**6a**), samples of the organic phase (50 μ L) were withdrawn after 2 and 24 h and used for derivatisation with dichloromethane (850 μ L), acetic acid anhydride (100 μ L), and pyridine (50 μ L) at RT for 1 h. The acetylated cyanohydrins were analysed with a 6890N gas chromatograph (Agilent Technologies) equipped with a PAL autosampler (CTC Analytics AG), a Varian CP7503, a CP-Chirasil-DEX CB column (25 m \times 320 μ m \times 0.25 μ m), and a flame ionization detector. GC parameters were as follows: carrier gas: constant pressure mode at 100 kPa H₂; injector: 250 °C. **1a**: Temperature programme: 60 °C, 10 °C min⁻¹ to 140 °C, 2 min at 140 °C; retention times: aldehyde 4.5 min, (*R*)-cyanohydrin acetate 9.6 min, (*S*)-cyanohydrin acetate 10.3 min; **2a**: temperature programme: 100 °C, 10 °C min⁻¹ to 125 °C, 1 °C min⁻¹ to 130 °C, 10 °C min⁻¹ to 170 °C, 1 min at 170 °C; retention times: aldehyde 2.0 min, (*R*)-cyanohydrin acetate 6.8 min, (*S*)-cyanohydrin acetate 7.1 min; **3a**: temperature programme: 100 °C, 10 °C min⁻¹ to 170 °C, 2 min at 170 °C; retention times: aldehyde 2.6 min, (*R*)-cyanohydrin acetate 6.2 min, (*S*)-cyanohydrin acetate 6.5 min; **4a**: temperature programme: 140 °C, 1 °C min⁻¹ to 150 °C, 10 °C min⁻¹ to 170 °C; retention times: aldehyde 1.9 min, (*R*)-cyanohydrin acetate 7.1 min, (*S*)-cyanohydrin acetate 9.3 min; **5a**: temperature programme: 105 °C, isotherm; retention times: aldehyde 0.8 min, (*S*)-cyanohydrin acetate 3.3 min, (*R*)-cyanohydrin acetate 4.6 min; **6a**: temperature programme: 110 °C, 0 min, 10 °C min⁻¹ to 130 °C, 20 °C min⁻¹ to 170 °C, 0.5 min at 170 °C; retention times: aldehyde 0.9 min, (*R*)-cyanohydrin acetate 2.5 min, (*S*)-cyanohydrin acetate 2.6 min.

Crystallization and structure determination of GtHNL-A40H/V42T/Q110H

Initial crystallization trials of GtHNL-A40H/V42T/Q110H were performed with an Oryx 8 robot (Douglas Instruments) by using the sitting drop method. Protein concentrations of 9 and 18 mg mL⁻¹ (in 20 mM TRIS-HCl, pH 7.0, 200 mM NaCl) were used. Drops of the enzyme solution (0.8 μ L) were mixed with the reservoir solution (0.8 μ L) by using JCSG-plus and Morpheus crystallization screens (Molecular Dimensions). All plates were incubated at 16 °C. Initial crystals were observed after 3 days under several conditions. Crystallization conditions were optimised, and a complete data set to 2.1 Å resolution was collected from the beamline ID23-2 at the European Synchrotron Radiation Facility (Grenoble)^[28] from a crystal obtained under condition 1.15 of the JCSG-plus screen (0.2 M sodium thiocyanate, 20% w/v polyethylene glycol 3350).

Data were processed by using the XDS program suite^[29] and software from the CCP4 suite.^[30] The structure was solved by molecular replacement using the program Phaser^[31] and the structure of GtHNL-WT [Protein Data Bank (PDB) entry 4bif] as the search template.^[7] Structure rebuilding and refinement were performed with Coot^[32] and Refmac5.^[33] The final structure was validated by using the program MolProbity.^[34] Atomic coordinates and structure factors were deposited in the PDB under the accession number 4UXA.

Thermal shift assay

The thermal shift assay was performed as described in the literature^[35] with an Applied Biosystems 7500 Fast Real-Time PCR system (Life Technologies) and 96-Well Optical Reaction plates. Each well contained purified protein (5 μ g; GtHNL-WT and variants) and 1X SYPRO Orange dye (Sigma–Aldrich) in various buffers

(100 mM citrate/phosphate buffer, pH 7.5–3.0, 100 mM sodium oxalate buffer, pH 7.5–3.0, 100 mM sodium acetate buffer, pH 5.5–4.0, added as 0.5 M stock, the protein storage buffer, 20 mM TRIS-HCl, 200 mM NaCl, pH 7.5 was used as a reference) and a total volume of 25 μ L. The temperature was increased from 20 to 95 °C (step size: 1 °C). The increase of the fluorescence of the SYPRO Orange probe during the unfolding of the protein was measured with excitation at 490 nm and emission at 575 nm. Measurements were performed in duplicate or triplicate.

Acknowledgements

This work has been supported by the Federal Ministry of Science, Research and Economy (BMWFW), the Federal Ministry of Traffic, Innovation and Technology (bmvit), the Styrian Business Promotion Agency SFG, the Standortagentur Tirol and ZIT—Technology Agency of the City of Vienna through the competence centers for excellent technologies (COMET) funding program managed by the Austrian Research Promotion Agency FFG. This project has received funding from the European Union's Seventh Framework Programme for research, technological development, and demonstration under grant agreement no. 289646 (KyroBio). We acknowledge the ESRF for the provision of synchrotron-radiation facilities and thank the ESRF scientific and technical personnel for assistance in using the beamline ID23-2. We thank Ing. Karin Reicher, MSc, for helping with cyanohydrin synthesis and protein purification and Sarah Trunk, MSc, for performing the thermal shift assay.

Keywords: biocatalysis • cupins • cyanohydrin syntheses • protein engineering • lyases

- [1] M. Gruber-Khadjawi, M. H. Fechter, H. Griengl in *Enzyme Catalysis in Organic Synthesis* (Eds.: K. Drauz, H. Gröger, O. May), Wiley-VCH, Weinheim, **2012**, pp. 947–990.
- [2] E. Lanfranchi, K. Steiner, A. Glieder, I. Hajnal, R. A. Sheldon, S. van Pelt, M. Winkler, *Recent Pat. Biotechnol.* **2013**, *7*, 197–206.
- [3] T. Purkarthofer, W. Skranc, C. Schuster, H. Griengl, *Appl. Microbiol. Biotechnol.* **2007**, *76*, 309–320.
- [4] M. Winkler, A. Glieder, K. Steiner, in *Comprehensive Chirality, Synthetic Methods VI—Enzymatic and Semi-Enzymatic*, Vol. 7 (Eds.: E. M. Carreira, H. Yamamoto), Elsevier, Amsterdam, **2012**, pp. 350–371.
- [5] J. N. Andexer, J. V. Langermann, U. Kragl, M. Pohl, *Trends Biotechnol.* **2009**, *27*, 599–607.
- [6] M. Dadashpour, Y. Asano, *ACS Catal.* **2011**, *1*, 1121–1149.
- [7] I. Hajnal, A. Łyskowski, U. Hanefeld, K. Gruber, H. Schwab, K. Steiner, *FEBS J.* **2013**, *280*, 5815–5828.
- [8] Z. Hussain, R. Wiedner, K. Steiner, T. Hajek, M. Avi, B. Hecher, A. Sessitsch, H. Schwab, *Appl. Environ. Biotechnol.* **2012**, *78*, 2053–2055.
- [9] R. Wiedner, M. Gruber-Khadjawi, H. Schwab, K. Steiner, *Comp. Struct. Biotechnol. J.* **2014**, *10*, 58–62.
- [10] A. Łyskowski, K. Steiner, I. Hajnal, G. Steinkellner, H. Schwab, K. Gruber, *Acta Crystallogr. Sect. F* **2012**, *68*, 451–454.
- [11] Y. Asano, M. Dadashpour, M. Yamazaki, N. Doi, H. Komeda, *Prot. Eng. Des. Sel.* **2011**, *24*, 607–616.
- [12] M. Avi, R. M. Wiedner, H. Griengl, H. Schwab, *Chem. Eur. J.* **2008**, *14*, 11415–11422.
- [13] J. von Langermann, D. M. Nedrud, R. J. Kazlauskas, *ChemBioChem* **2014**, *15*, 1931–1938.
- [14] D. Okrob, J. Metzner, W. Wiechert, K. Gruber, M. Pohl, *ChemBioChem* **2012**, *13*, 797–802.
- [15] A. Glieder, R. Weis, W. Skranc, P. Pöchlauer, I. Dreveny, S. Majer, M. Wubolts, H. Schwab, K. Gruber, *Angew. Chem. Int. Ed.* **2003**, *42*, 4815–4818; *Angew. Chem.* **2003**, *115*, 4963–4966.
- [16] Z. Liu, B. Pscheidt, M. Avi, R. Gaisberger, F. S. Hartner, C. Schuster, W. Skranc, K. Gruber, A. Glieder, *ChemBioChem* **2008**, *9*, 58–61.
- [17] B. Pscheidt, Z. B. Liu, R. Gaisberger, M. Avi, W. Skranc, K. Gruber, H. Griengl, A. Glieder, *Adv. Synth. Catal.* **2008**, *350*, 1943–1948.
- [18] R. Weis, R. Gaisberger, W. Skranc, K. Gruber, A. Glieder, *Angew. Chem. Int. Ed.* **2005**, *44*, 4700–4704; *Angew. Chem.* **2005**, *117*, 4778–4782.
- [19] B. Krammer, K. Rumbold, M. Tschemmerneegg, P. Pöchlauer, H. Schwab, *J. Biotechnol.* **2007**, *129*, 151–161.
- [20] J. Andexer, J. von Langermann, A. Mell, M. Bocola, U. Kragl, T. Eggert, M. Pohl, *Angew. Chem. Int. Ed.* **2007**, *46*, 8679–8681; *Angew. Chem.* **2007**, *119*, 8833–8835.
- [21] W. Skranc, A. Glieder, K. Gruber, R. Weis, O. Maurer, R. Gaisberger, WO2006076965.
- [22] W. Skranc, A. Glieder, K. Gruber, R. Weis, R. Luiten, WO2004083424 B2.
- [23] W. Becker, E. Pfeil, *Biochem. Z.* **1965**, *346*, 301–321.
- [24] D. Balzer, G. Ziegelin, W. Pansegrau, V. Kruft, E. Lanka, *Nucl. Acids Res.* **1992**, *20*, 1851–1858.
- [25] O. Edelheit, A. Hanukoglu, I. Hanukoglu, *BMC Biotechnol.* **2009**, *9*, 61.
- [26] E. Gasteiger, C. Hoogland, A. Gattiker, S. Duvaud, M. R. Wilkins, R. D. Appel, A. Bairoch in *The Proteomics Protocols Handbook* (Ed.: J. M. Walker), Humana Press, **2005**, pp. 571–607.
- [27] D. Okrob, M. Paravidino, R. V. A. Orru, W. Wiechert, U. Hanefeld, M. Pohl, *Adv. Synth. Catal.* **2011**, *353*, 2399–2408.
- [28] D. Flot, T. Mairs, T. Giraud, M. Guijarro, M. Lesourd, V. Rey, D. van Brussel, C. Morawe, C. Borel, O. Hignette, J. Chavanne, D. Nurizzo, S. McSweeney, E. Mitchell, *J. Synchr. Rad.* **2010**, *17*, 107–118.
- [29] W. Kabsch, *Acta Crystallogr. Sect. D* **2010**, *66*, 125–132.
- [30] M. D. Winn, C. C. Ballard, K. D. Cowtan, E. J. Dodson, P. Emsley, P. R. Evans, R. M. Keegan, E. B. Krissinel, A. G. W. Leslie, A. McCoy, S. J. McNicholas, G. N. Murshudov, N. S. Pannu, E. A. Potterton, H. R. Powell, R. J. Read, A. Vagin, K. S. Wilson, *Acta Crystallogr. Sect. D* **2011**, *67*, 235–242.
- [31] A. J. McCoy, R. W. Grosse-Kunstleve, P. D. Adams, M. D. Winn, L. C. Storoni, R. J. Read, *J. Appl. Crystallogr.* **2007**, *40*, 658–674.
- [32] P. Emsley, K. Cowtan, *Acta Crystallogr. Sect. D* **2004**, *60*, 2126–2132.
- [33] G. N. Murshudov, A. A. Vagin, E. J. Dodson, *Acta Crystallogr. Sect. D* **1997**, *53*, 240–255.
- [34] V. B. Chen, W. B. Arendall, J. J. Headd, D. A. Keedy, R. M. Immormino, G. J. Kapral, L. W. Murray, J. S. Richardson, D. C. Richardson, *Acta Crystallogr. Sect. D* **2010**, *66*, 12–21.
- [35] U. B. Ericsson, B. M. Hallberg, G. T. DeTitta, N. Dekker, P. Nordlund, *Anal. Biochem.* **2006**, *357*, 289–298.

Received: September 15, 2014

Published online on December 3, 2014